A NEW FILTERED DYNAMIC SUBGRID-SCALE MODEL FOR LARGE EDDY SIMULATION OF INDOOR AIRFLOW

Wei Zhang and Qingyan Chen
Building Technology Program
Massachusetts Institute of Technology
77 Mass. Ave., Cambridge, MA 02139-4307, USA

ABSTRACT

Large Eddy Simulation (LES) with a Dynamic Subgrid-scale Model (DSM) is a powerful tool to predict indoor airflow. However, the model needs to average the model coefficient over a homogeneous direction. Since most indoor airflow does not have a homogeneous direction, this study proposed a new Filtered Dynamic Subgrid-scale Model (FDSM) without the need of a homogeneous flow direction. The predicted air velocity, air temperature and turbulence distributions agree reasonably well with the experimental data. The results show that the FDSM can be used to simulate indoor airflow.

INTRODUCTION

To design a comfortable and healthy indoor environment, one requires information about the distributions of air velocity, air temperature, relative humidity, contaminant concentrations, and turbulent quantities. These information can be obtained numerically by using a Computational-Fluid-Dynamics (CFD) program with a eddy viscosity model. However, the power spectrum of airflow may play an important role in thermal comfort. The power spectrum can only be calculated by Large Eddy Simulation (LES) at present. The LES model should be a next-generation tool to study indoor airflow in buildings, because it is universal, has few or no adjustable model coefficients, can provide more flow information, and can calculate flow that is difficult to be determined by other CFD models. For example, with an eddy-viscosity model, the mean airflow through a window over time would close to zero for natural ventilation under isothermal conditions. However, an LES simulation can correctly predict the instantaneous airflow through the window.

Typical indoor airflow includes natural convection, such as winter heating by a baseboard heater; forced convection, such as free cooling in shoulder seasons; and mixed convection, such as summer cooling with an air conditioner. The indoor airflow is complex and is driven by pressure gradients and thermal buoyancy. Very few LES studies on indoor airflow have been reported (Davidson and Nielsen 1996, Emmerich, and McGrattan 1998, Murakami et al. 1995). The results by LES do not agree very well with the experimental data probably due to a constant model coefficient used in the Smagorinsky model. Dynamic Subgrid-scale Model (DSM, Germano et al. 1991) is available to calculate the model coefficient as a function of time, space, and flow type. The model requires to average the coefficient over a homogeneous flow direction because the coefficient fluctuates significantly. It is possible to reduce the fluctuation by averaging the coefficient through a filter, which will be discussed extensively in this paper. In addition, for indoor airflow, it is difficult to find a homogeneous flow direction. It is necessary to find a simple method to determine the DSM coefficient for indoor airflow.

This investigation proposes a Filtered Dynamic Subgrid-scale Model (FDSM) to determine the model coefficient for flow without a homogeneous direction. The FDSM has been applied to natural and mixed convection flows. The corresponding experimental data available from the literature and the computed results with the DSM have been compared to examine if the FDSM can correctly predict indoor airflow.

THE DYNAMIC SUBGRID-SCALE MODEL (DSM)

The LES requires the separation of small-eddies from large-eddies with a filter. For simplicity, the following section uses one-dimensional notation. The filtered velocity is:

$$\overline{u_i} = \int G(x, x')u_i(x)dx' \qquad (1)$$

where G(x, x') is a filter function. The filter function is large only when G (x, x') is less than the filter width, a length scale over which averaging is performed. The flow eddies larger than the filter width are "large-eddies" and smaller than the width are 'small-eddies'.

In the physical spaces, the paper uses a box filter, i.e.:

$$G(x_i) = \begin{cases} \dfrac{1}{\Delta_i} & (|x_i| \le \dfrac{\Delta_i}{2}) \\ 0 & (|x_i| > \dfrac{\Delta_i}{2}) \end{cases}, \qquad (2)$$

With the finite volume method, it seems natural to define the filter width, Δ_i, as an average over a grid volume.

With the filter, it is possible to derive the governing conservation equations for the momentum (Navier-Stokes equations), mass continuity, and energy. The filtered Navier-Stokes equations for an incompressible flow are:

$$\frac{\partial \overline{u_i}}{\partial t}+\frac{\partial}{\partial x_j}(\overline{u_i}\cdot\overline{u_j})=-\frac{1}{\rho}\frac{\partial \overline{P}}{\partial x_i}+ \upsilon\frac{\partial^2 \overline{u}_i}{\partial x_i\,\partial x_j}-\frac{\partial \tau_{ij}}{\partial x_j}+g_j\beta(\overline{\theta}-\theta_0)\delta_{ij} \quad (3)$$

where the subgrid Reynolds stresses are

$$\tau_{ij}=\overline{u_i u_j}-\overline{u_i}\cdot\overline{u_j} \quad (4)$$

LES also solves the filtered energy equation with subgrid heat fluxes with heat transfer problem:

$$h_j=\overline{u_j\theta}-\overline{u}_j\,\overline{\theta} \quad (5)$$

The terms, $\overline{u_i u_j}$, and $\overline{u_j\theta}$, are unknown and need to be modeled.

Dynamic Subgrid-Scale Model. The Reynolds stresses can be modeled using the Smagorinsky model in order to close the equations. The Smagorinsky model uses a constant model coefficient that depends on the flow type. On the other hand, Germano et al. (1991) proposed a dynamic subgrid-scale model (DSM). The DSM calculates the model coefficient by relating the subgrid scale Reynolds stresses to two different sizes of filters. Since the Reynolds stresses vary with time and location, the resulting model coefficient is therefore a function of time and location.

The DSM uses an explicit test filter, $\tilde{G}$, with a filter width of $\tilde{\Delta}$ ($\tilde{\Delta}>\overline{\Delta}$) to determine the turbulent stresses on the $\tilde{G}$ filter:

$$T_{ij}=\widetilde{\overline{u_i u_j}}-\tilde{\overline{u}}_i\tilde{\overline{u}}_j \quad (6)$$

The first term on the right side of the equation cannot be determined directly, as that in Eq. (4). However, substituting Eq. (6) from the Eq. (4) with a test filter can eliminate the term:

$$T_{ij}-\tilde{\tau}_{ij}=L_{ij} \quad (7)$$

$$L_{ij}=\widetilde{\overline{u}_i\overline{u}_j}-\tilde{\overline{u}}_i\tilde{\overline{u}}_j \quad (8)$$

where

The resolved turbulent stresses in Eq. (8), L_{ij}, can be calculated explicitly. With the definition of the Smagorinsky model, the stresses of the test filter, T_{ij}, and that of the grid filter, τ_{ij}, are:

$$\tau_{ij}-\frac{\delta_{ij}}{3}\tau_{kk}=-2C_\tau\overline{\Delta}^2\left|\overline{S}\right|\overline{S}_{ij}=-C_\tau\beta_{ij} \quad (9)$$

$$T_{ij}-\frac{\delta_{ij}}{3}T_{kk}=-2C_T\tilde{\Delta}^2\left|\tilde{\overline{S}}\right|\tilde{\overline{S}}_{ij}=-C_T\alpha_{ij} \quad (10)$$

where $\overline{\Delta}$ is the grid filter width and $\tilde{\Delta}$ the test filter width. The C_τ and C_T are the coefficients of the grid and test filters, respectively. Further,

$$\tilde{\overline{S}}_{ij}=\frac{1}{2}\left(\frac{\partial\tilde{\overline{u}}_i}{\partial x_j}+\frac{\partial\tilde{\overline{u}}_j}{\partial x_i}\right),\qquad \left|\tilde{\overline{S}}\right|=\sqrt{2\tilde{\overline{S}}_{ij}\tilde{\overline{S}}_{ij}} \quad (11)$$

Substitution of (9) and (10) into (7) gives:

$$L_{ij}-\frac{1}{3}\delta_{ij}L_{kk}=C_T\,\alpha_{ij}-C_\tau\,\beta_{ij} \quad (12)$$

where $\alpha_{ij}=2\tilde{\Delta}^2\left|\tilde{\overline{S}}\right|\tilde{\overline{S}}_{ij}$ and $\beta_{ij}=2\overline{\Delta}^2\left|\overline{S}\right|\overline{S}_{ij}$. The C_τ in (12) cannot be solved explicitly because it is in the test filtering operation. Germano et al. (1991) extracted the C from the filtering operation, and assumed:

$$C\approx C_\tau\approx C_T \quad (13)$$

$$C_\tau\beta_{ij}=C_\tau\tilde{\beta}_{ij} \quad (14)$$

Using the least-square approach suggested by Lilly (1992), the C can be solved via

$$C=\frac{<L_{ij}M_{ij}>}{<M_{ij}M_{ij}>} \quad (15)$$

where $M_{ij}=(\alpha_{ij}-\tilde{\beta}_{ij})$, and $<\ >$ denotes a plane averaging over a homogeneous direction. Without an average over the homogenous direction, the C fluctuates a lot and that makes the solution of the flow very unstable. The averaging procedure can dampen large fluctuations of the C often encountered in a flow prediction. This procedure gives good results for simple flows with at least one homogeneous direction, such as a turbulent channel flow. However, the averaging procedure cannot be used for a flow without a homogeneous direction.

Similarly, Lilly (1992) modeled the subgrid-scale heat fluxes ($h_j=\overline{u_j\theta}-\overline{u}_j\,\overline{\theta}$) with a simplified Boussinesq approximation to determine the subgrid-scale Prandtl number (Pr_{SGS}),

$$\frac{1}{Pr_{SGS}}=\frac{1}{2C}\frac{P_jR_j}{R_j^2} \quad (16)$$

where,

$$P_j=\widetilde{\overline{u}_j\theta}-\tilde{\overline{u}}_j\,\tilde{\overline{\theta}} \quad (17)$$

$$R_j=\tilde{\overline{\Delta}}^2\left|\tilde{\overline{S}}\right|\frac{\partial\tilde{\overline{\theta}}}{\partial x_j}-\widetilde{\overline{\Delta}^2\left|\overline{S}\right|\frac{\partial\overline{\theta}}{\partial x_j}} \quad (18)$$

Filtered Dynamic Subgrid-Scale Model. Since most indoor airflow does not have a homogeneous direction. This paper proposes a simple method to determine the model coefficient in the DSM by using a localized filter technique. It is done by applying a grid filter to Eq. (7). The use of the grid filter is to average the coefficient and to smooth the large fluctuation of the coefficient. The technique will lead to a stable numerical solution. Then all the terms in Eq. (7) will be related to the grid filter:

$$\overline{T}_{ij} - \overline{\tilde{\tau}}_{ij} = \overline{L}_{ij} \qquad (19)$$

Replacement of τ_{ij} and T_{ij} in Eq. (19) with a model, such as the Smagorinsky model or the mixed model (Zang et al, 1993), gives rise to an error in satisfying Eq. (19). The error associated with a model τ_{ij}^{model} is given by

$$e_{ij} = \overline{L}_{ij} - (\overline{T}_{ij}^{model} - \overline{\tilde{\tau}}_{ij}^{model}) \qquad (20)$$

For simplicity, the use of the Smagorinsky model leads to the following error equation:

$$e_{ij} = \overline{L}_{ij} - \overline{2 C_T \tilde{\Delta}^2 \left|\tilde{\bar{S}}\right| \tilde{\bar{S}}_{ij}} + \overline{2 C_\tau \bar{\Delta}^2 \left|\bar{S}\right| \bar{S}}_{ij} \qquad (21)$$

Using the definitions of $\alpha_{ij} = 2\tilde{\Delta}^2 \left|\tilde{\bar{S}}\right| \tilde{\bar{S}}_{ij}$ and $\beta_{ij} = 2\bar{\Delta}^2 \left|\bar{S}\right| \bar{S}_{ij}$, Eq. (21) can be re-written as:

$$e_{ij} = \overline{L}_{ij} - \overline{C_T \alpha_{ij}} + \tilde{C}_\tau \beta_{ij} \qquad (22)$$

If we assume:

$$\overline{C_T \alpha_{ij}} \approx \overline{C}_T \overline{\alpha}_{ij}, \qquad (23)$$

$$\tilde{C}_\tau \beta_{ij} \approx \overline{\tilde{C}}_\tau \overline{\tilde{\beta}}_{ij} \qquad (24)$$

$$C \approx \overline{\tilde{C}}_\tau \approx \overline{C}_T. \qquad (25)$$

Then the equation becomes

$$e_{ij} = \overline{L}_{ij} - \overline{C_T \alpha_{ij}} + \tilde{C}_\tau \beta_{ij} = \overline{L}_{ij} - C\overline{M}_{ij} \qquad (26)$$

where $M_{ij} = \alpha_{ij} - \tilde{\beta}_{ij}$.

The following paragraphs discuss the assumptions used in Eq.(22) to (25).

Meneveau et al. (1996) used DNS data to analyze the two hypotheses in Eqs.(13) and (14). They filtered DNS data at both a grid filter and test filter and compared the coefficients obtained with and without the time averaging procedure. Although the two coefficients are not equal without averaging, they are similar with the time averaging:

$$C^{DNS}{}_\tau \neq C^{DNS}{}_T \qquad (27)$$

$$\{C^{DNS}{}_\tau\} \approx \{C^{DNS}{}_T\} \qquad (28)$$

where {} denotes the time averaging. Meneveau et al. (1996) also discussed the minimization error caused by approximating $\tilde{C}_\tau \beta_{ij} = \overline{\tilde{C}}_\tau \overline{\tilde{\beta}}_{ij}$ with and without using the averaging technique. The study shows that the minimization error with the averaging is smaller than that without the averaging:

$$\text{Error}_{\min}(\{\overline{\tilde{C}}_\tau \overline{\tilde{\beta}}_{ij}\}, \{\tilde{C}_\tau \beta_{ij}\}) \ll \text{Error}_{\min}(\overline{\tilde{C}}_\tau \overline{\tilde{\beta}}_{ij}, \tilde{C}_\tau \beta_{ij}) \qquad (29)$$

Since the filtering is also a kind of averaging technique, the results obtained by Meneveau et al. (1996) may be extended to the grid filtering technique. Therefore, the assumptions used in Eqs. (23), (24), and (25) should be valid. These assumptions should be better than those used in DSM (Eqs. (13) and (14)).

Localization of the Coefficient with Least-Square Approach. The present investigation uses the least-square approach to obtain the localized coefficient, the C in Eq. (26), as suggested by Lilly (1992). At any given point in a space, **x**, the e_{ij} is a function of the C but depends on the **x**. In order to obtain an optimal C, the e_{ij} must be integrated over the entire flow domain. On the other hand, the least-square approach requires the optimization over the entire flow domain. However, the square of the residual, $e_{ij}e_{ij}$, may have a locally violent change. The $e_{ij}e_{ij}$ should be integrated in the entire flow domain with a smooth function. Thus, the integrated square of the error function, $E_{ij}(C)$, is

$$E_{ij}(C) = \int G(\mathbf{x},\mathbf{x}') e_{ij}(\mathbf{x}') e_{ij}(\mathbf{x}') d\mathbf{x}' \qquad (30)$$

Substitute Eq. (23) into Eq.(27), and Eq. (27) reads:

$$E_{ij}(C) = \int G(\mathbf{x},\mathbf{x}') (\overline{L}_{ij} - C\overline{M}_{ij})^2 d\mathbf{x}' \qquad (31)$$

Since the least square condition for the Eq.(31) is $\frac{\partial E_{ij}(C)}{\partial C} = 0$, then the optimal model coefficient C is obtained as:

$$C = \frac{\int G(\mathbf{x},\mathbf{x}') \overline{L}_{ij} \overline{M}_{ij} d\mathbf{x}'}{\int G(\mathbf{x},\mathbf{x}') \overline{M}_{ij} \overline{M}_{ij} d\mathbf{x}'} \qquad (32)$$

The C is obviously a function of time and space and is inconsistent with the definition given by Germano et al. (1991). The C here seems superior to the one proposed by Germano et al. (1991), because it can be applied to inhomogeneous flows.

The smooth function G (***x***, ***x***') should be chosen for the entire flow domain and may depend on the turbulent scales. Although the smooth function can be in many forms, a box filter may be the most convenient. The filter can be either a grid filter or a test filter:

$$C = \frac{\overline{\overline{L}_{ij} \overline{M}_{ij}}}{\overline{\overline{M}_{ij} \overline{M}_{ij}}} \qquad \text{(with the grid filter)} \qquad (33)$$

or

$$C = \frac{\overline{L}_{ij} \overline{M}_{ij}}{\overline{M}_{ij} \overline{M}_{ij}} \qquad \text{(with the test filter)} \qquad (34)$$

Eqs. (33) and (34) are now defined as the Filtered Dynamic Subgrid-scale Model (FDSM). The $FDSM\text{-}_G$ is with grid filter for Eq. (33) and $FDSM_T$ with test filter for Eq.(34). The FDSM is much simpler than those proposed by Ghosal et al. (1995) and Meneveau et al. (1996).

The FDSM-$_G$ or FDSM-$_T$ can also be locally negative. A negative C indicates a negative eddy viscosity and implies an energy transfer from small scales to the resolved scales or backscatter, according to Piomelli et al.(1991). However, the negative C can also lead to numerical instability. In order to avoid the instability, the present investigation uses

C = max (0.0, Eq.(33) or (34)) (35)

Similarly, we can also calculate the Prandtl number of the dynamic subgrid heat fluxes by:

$$\frac{1}{Pr_{SGS}} = \frac{1}{2C}\frac{\overline{\overline{P}_j\overline{R}_j}}{\overline{\overline{R}_j\overline{R}_j}} \text{ (with the grid filter)} \qquad (36)$$

or

$$\frac{1}{Pr_{SGS}} = \frac{1}{2C}\frac{\tilde{\overline{P}}_j\tilde{\overline{R}}_j}{\tilde{\overline{R}}_j\tilde{\overline{R}}_j} \text{ (with the test filter)} \qquad (37)$$

APPLICATIONS TO INDOOR AIRFLOW

To demonstrate the ability of the new FDSM, the model is used to calculate several typical airflows in rooms:

- ☞ natural convection in a room with a heated wall and a cooled wall
- ☞ mixed convection in a room with a heated floor and a cold air jet near the ceiling

Natural Convection. The investigation has selected the natural convection flow in a cavity as shown in Fig. 1(a). Cheesewright (1986) measured the air velocity, temperature, turbulence energy, and heat transfer in the cavity. The flow characteristics of the cavity are similar to those in a room. The simple geometry eliminates many potential errors, such as those caused by the complex geometry of a baseboard heater. If there are discrepancies between the computed results and measured data, this would allow us to identify the reasons.

Since natural convection consists of both turbulent and laminar flows, it is very challenging to use LES to simulate the flows. This case enables us to use the DSM, which can be averaged over the depth direction. The depth direction can be considered homogeneous. The LES with the DSM and FDSM (FDSM-G, FDSM-T) is used to predict the distributions of air velocity, temperature, and turbulence energy.

Fig. 1(a) shows the cavity geometry (height AC=2.5 m, width AB=0.5 m, and the depth is 0.5 m) as well as the numerical grid distribution used in the LES simulations. The temperature difference between the warm and cold walls, $\Delta\theta$, is 45.8 K (left wall temperature, θ_1, is 68.0°C, and right wall temperature, θ_2, is 22.2°C). All of the other walls were insulated. The flow corresponds to a Rayleigh number (Ra) of 5.0×10^{10}, similar to that found in a typical room. The Ra is defined as

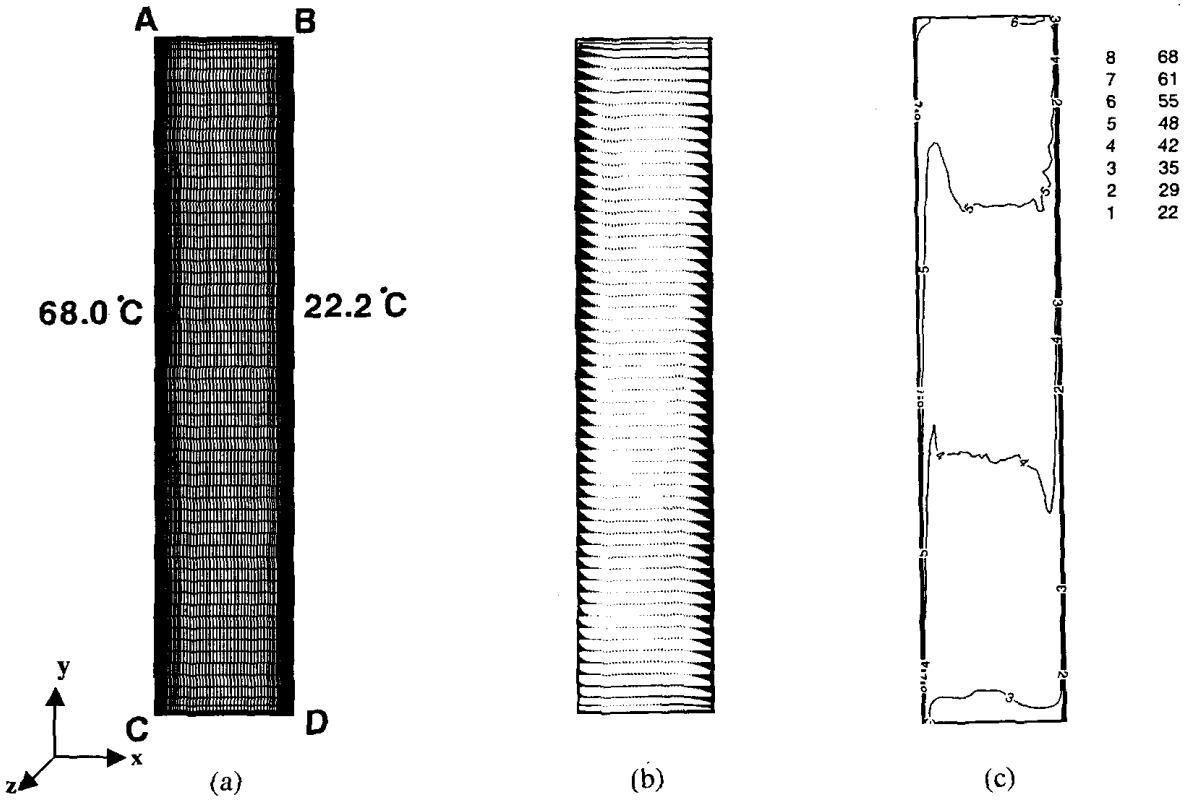

Fig. 1 The predicted results of the natural convection in a cavity with the FDSM-G at depth =0.25 m.
(a) The cavity geometry, (b) average air velocity, (c) average air temperature.

$$Ra = \frac{(\theta_1 - \theta_2)\, gH^3}{\upsilon\alpha} \qquad (38)$$

The computations used no-slip velocity conditions for all the walls. The mesh employed were $62\times62\times12$ for the height (X), width (Y), and depth (Z) directions, respectively, and the time step Δt =0.0002 s.

The initial air velocity was zero and air temperature 45.1 °C for the whole flow domain. When the flow became statistically steady, the averaging technique was used to obtain the mean value of the computed parameters, such as air velocity and temperature. The averaging time is about 120 s.

Figs. 1(b), 1(c) show the distributions of average air velocity, average air temperature with FDSM-G on the center section (depth is 0.25 m), respectively. The velocity field is asymmetric. The hot wall generates an upward flow near the wall and the cold wall a downward flow. The velocity in the center of the cavity is generally small. The flow is laminar in the lower part of the hot wall and the upper part of the cold wall.

Fig. 2 compares the predicted and measured results in the span-wise of the cavity. The results with the DSM (averaging in the depth direction), the FDSM-$_G$ and the FDSM-$_T$ agree rather well with the experimental data except near the wall regions. However, the FDSM-$_G$ and FDSM-$_T$ can predict flow without averaging along a homogeneous direction. This is very important because there is no homogeneous direction in most rooms with natural convection.

As reported by Cheesewright (1986), the top and bottom walls of the cavity were not well insulated. The heat loss in the lab environment led to a lower mean air temperature in the cavity. As a result, the predicted mean air temperature in the cavity is higher than the measured data as illustrated in Fig. 2(b). All models predicted a reasonably good temperature profile.

The present investigation calculates the turbulence energy as $k = (u'^2+v'^2+w'^2)/2$ (grid scale). Fig. 2(c) compares the computed k profiles with the experimental data. The DSM model under-predicts the turbulence energy near the walls. The performance of the FDSM-$_G$ and FDSM-$_T$ are similar to that of the DSM, although they still under-predict the turbulence energy, especially near the walls. The reason may be attributed to the *ad hoc* fix for the coefficient C ($C\geq0.0$).

This case shows that the FDSM-$_G$ and FDSM-$_T$ have the same performance as the DSM. Since the FDSM-$_G$ and FDSM-$_T$ do not need averaging over a homogeneous direction, they can be used to calculate more complex airflow. When comparing the FDSM-G and FDSM-$_T$, the FDSM-$_G$ is slightly better than the FDSM-$_T$.

Mixed Convection. The present investigation also applied the FDSM for mixed convection flow in a room, as shown in Fig. 3(a). Blay et al. (1992) measured the air velocity, temperature, and turbulent energy distributions for the case. The geometry of the test rig was H = 1.04 m long, L = 1.04 m wide, and D = 0.7 m deep. This is a scale-model of a room and has a homogeneous direction (the depth direction) so that the DSM can also be used. The inlet height, h_{in}, was 0.018 m, the supply air velocity, U_{in}, was 0.57 m/s, and the supply air temperature, T_{in}, was 15°C. The outlet height was 0.024m. The test rig used a floor heating system with a floor temperature, T_f, of 35°C. All other wall temperatures, T_w, were 15°C. The corresponding Archimedes number ($Ar = \frac{\beta g h_{in}\, \Delta T}{U_{in}^2}$) is 0.0036 and the Reynolds number ($Re = \frac{U_{in} h_{in}}{\nu}$) is 678.

The computations used a non-slip velocity condition for all the walls. The meshes employed were $62\times62\times12$ for the height (X), width (Y), and depth (Z) directions, respectively.

Figs. 3(b) and 3(c) show the measured mean air velocity distribution and the averaged air velocity distribution using the FDSM-$_G$. The airflow patterns are almost the same between the measurements and computations. The LES simulation shows a small re-circulation in the left-bottom corner, but not in the experiment. It is not clear if this is due to insufficient fine measuring points or due to the numerical model used.

Figs. 4 and 5 further compares the predicted mean air velocity, temperature, and turbulent energy distributions using the DSM, FDSM-$_G$ and FDSM-$_T$ with the experimental data at two center sections at X = 0.502 m and Y = 0.502 m. Figs. 4(a) and 5 (a) show that the three subgrid-scale models give very similar air velocity profiles. The FDSM-$_G$ is slightly better than the others. The predicted velocity profiles agree reasonably well with the experimental data.

However, Figs. 4(b) and 5(b) indicate that the predicted air temperature using the three models is about 1.5 K higher than the measured one, though the shape of the predicted temperature profiles is the same as the measured one. The models may over-predict the heat transfer from the floor or under-predict the heat transfer to the other walls. Since no detailed measurements on the heat transfer were available, it is difficult to identify the actual cause of the discrepancies. Perhaps the subgrid-scale Prandtl number was not correctly modeled for the buoyancy effect.

Figs. 4(c) illustrates that the computed turbulent energy ($k^{1/2} = \{(u'^2+v'^2+w'^2)/2\}^{1/2}$) profiles at section X = 0.502 m and the comparison with the corresponding experimental data. The FDSM-$_G$ and DSM can predict the turbulence energy distribution well, while the performance of the FDSM-$_T$ was poor. At section Y = 0.502 m, all three models over-predicted the turbulence energy as shown in Fig. 5(c). The models need to be developed further to predict the buoyancy effect correctly.

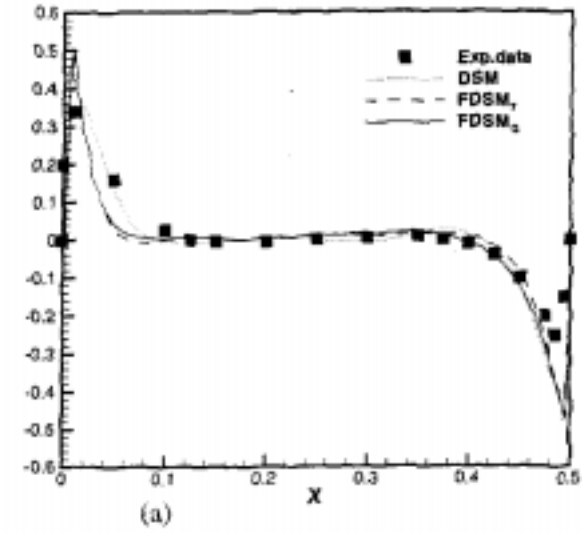

(a)

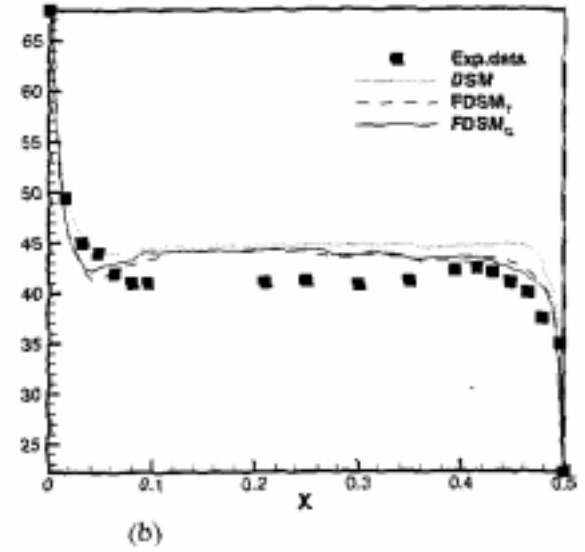

(b)

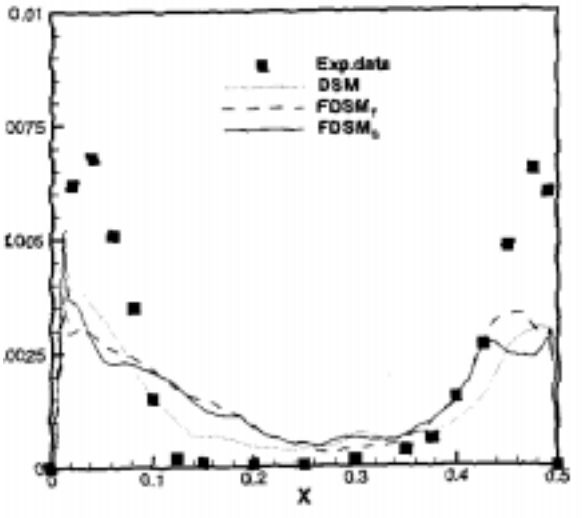

Fig. 2 Comparison of the predicted and measured results at mid height of the cavity. (a) average air velocity, (b) average air temperature, (c) average turbulent energy.

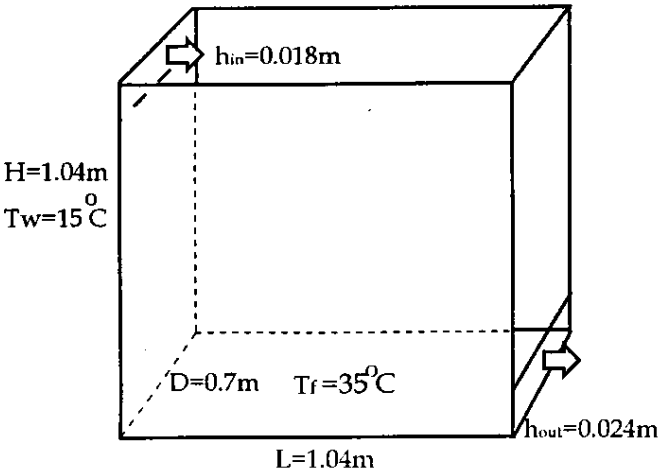

(a)

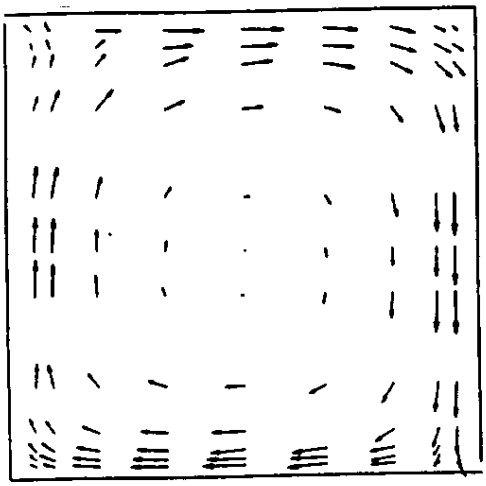

(b)

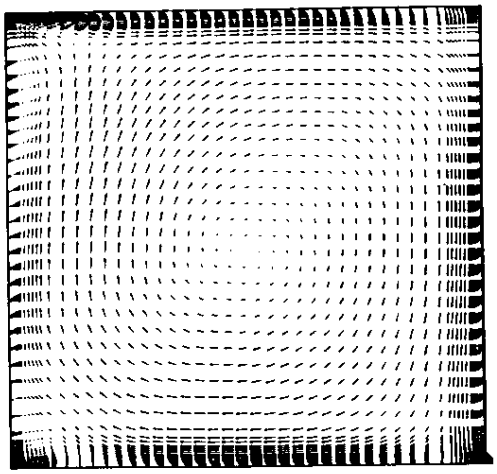

(c)

Fig. 3 The predicted and measured mixed convection flow in a room. (a) room geometry, (b) average velocity vectors obtained from the experiment (Baly et al,1992), (c) average velocity vectors computed by the FDSM-G

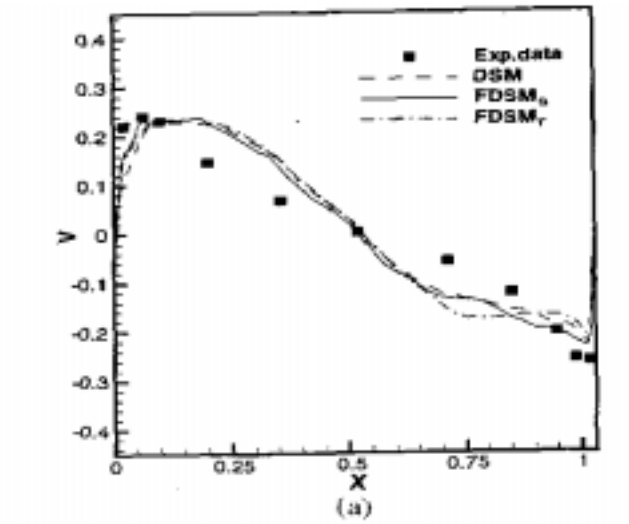

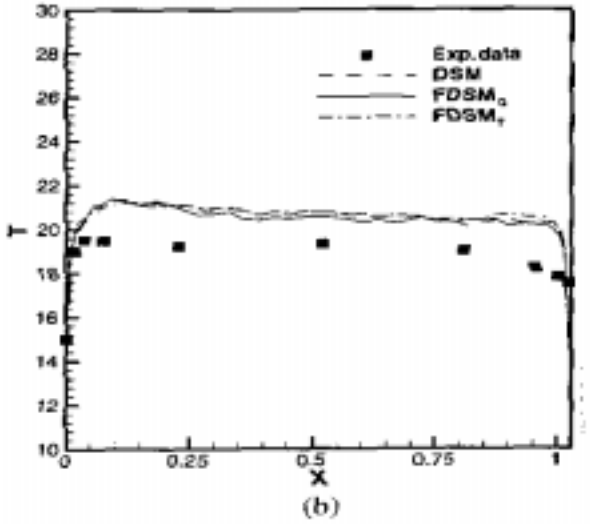

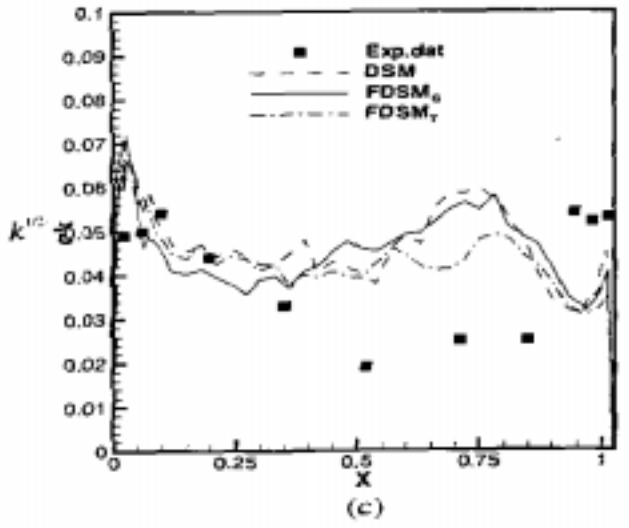

Fig. 4 Comparison of the predicted and measured results on the center sections (X=0.502m). (a) average velocity, (b) average temperature, (c) average turbulent energy ($k^{1/2}$).

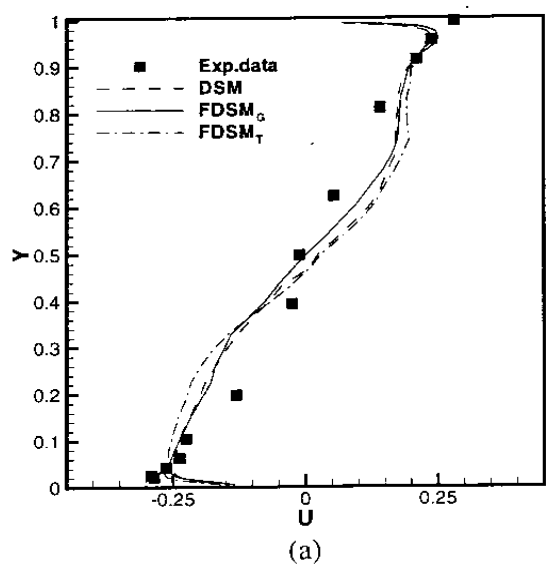

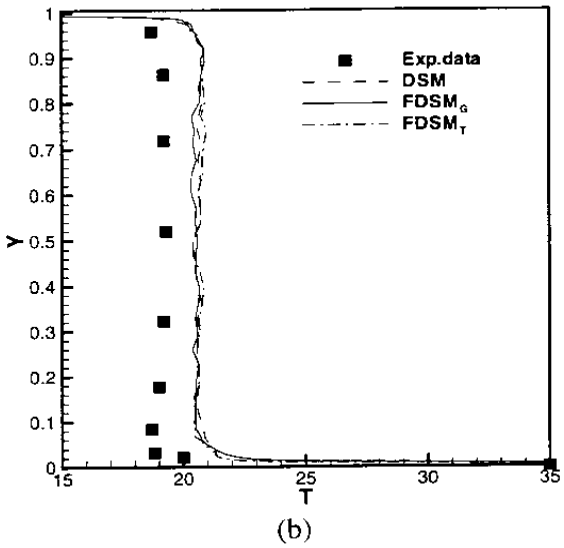

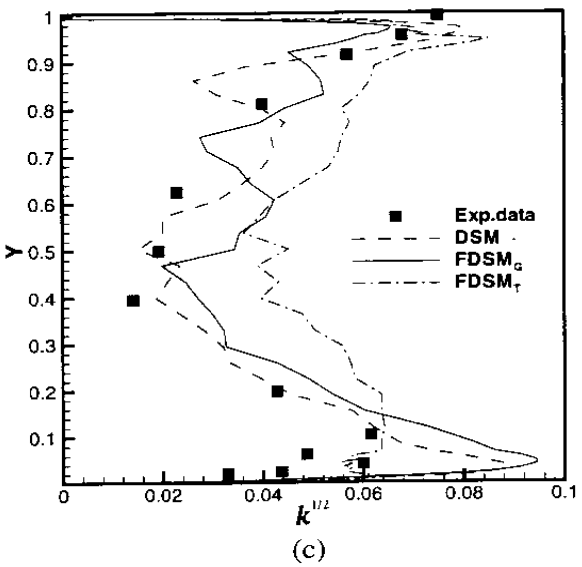

Fig. 5 Comparison of the predicted and measured results on the center sections (Y=0.502m). (a) average velocity, (b) average temperature, (c) average turbulent energy ($k^{1/2}$).

The reason for developing the new model is to calculate indoor airflow without a homogeneous flow direction. However, we have not found suitable experimental or direct-numerical-simulation data for this type of flow from the literature, although the flow exists in most rooms. Validation of the model needs detailed information of Reynolds stresses and heat fluxes. Further research in the direction is needed.

CONCLUSION

This study has developed a new filtered dynamic subgrid-scale model (FDSM) for large eddy simulation of complex flow without a homogeneous direction.

The model has been used to predict natural and mixed convection flow in a room. The computed results are compared with the experimental data available from the literature and those with the dynamic subgrid-scale model (DSM). The FDSM can correctly predict the average air velocity and temperature distributions in the room without a homogenous direction. However, it is more difficult to calculate the heat transfer near a wall and the turbulence energy distribution in the room. The models need to be developed further to predict the buoyancy effect correctly. The performance of the FDSM is the same as that of the DSM, but can be used for inhomogeneous flows, such as more complicated airflow in a room.

NOMENCLATURE

Ar :	Archimedes number
C:	DSM coefficient ($C=Cs^2$)
Cs:	Smagorinsky model coefficient
D:	Room depth
$G(x_i)$:	Filter function
g:	Gravitational acceleration
H:	Room height
L:	Room width
$\overline{p}_i$:	Grid filtered pressure
Pr:	Molecular prandtl number
Pr_{SGS}:	Subgrid-scale prandtl number
Ra:	Rayleigh number
T:	Temperature
u_i **:**	Velocities
$\overline{u}_i$ **:**	Grid filtered velocities
$\tilde{u}_i$:	Test filtered velocities
v:	Velocity vector
x_i :	Cartesian space coordinate
β :	Thermal expansion coefficient
θ:	Tempearture
ΔT :	Dimensionless time step
Δt :	Time step
Δ:	Filter size
ν:	Kinematic viscocity

ACKNOWLEDGMENT

The research was supported by the Center for Indoor Air Research.

REFERENCES

Blay, D., S. Mergui, and C. Niculae "Confined turbulent mixed convection in the presence of a horizontal buoyant wall jet " ASME HTD-Vol.213, Fundamentals of Mixed Convection, pp. 65-72, 1992.

Cheesewright, R., K.J. King,and S. Ziai " Experimental data for the validation of computer codes for the prediction of two-dimensional buoyant cavity flows, HTD-60, ASME Winter Annual Meeting, Anaheim, p.75, 1986.

Davidson, L. and P.V. Nielsen " Large Eddy Simulation of the flow in a three-dimensional ventilated room." Preceding of 5th International conference on air distribution in rooms ROOMVENT'96, pp. 161-168, 1996.

Emmerich, S.J. and K. B. McGrattan " Application of a Large Eddy Simulation model to study room airflow " ASHRAE Transactions, **104**, 1998.

Germano, M. U. Piomelli, P. Moin, and W. H. Cabot, "A dynamic subgrid-scale eddy viscosity model," J. Physics Fluids A **3,** 1760, 1991.

Ghosal, S., T. Lund, P. Moin, and K. Akselvoll, "A dynamic localization model for large-eddy simulation of turbulent flows, " J. Fluid Mechanics 286**,** 229, 1995.

Lilly, D.K. "A proposed modification of the Germano subgrid-scale closure method," J. Physics Fluids A, **4**, 633, 1992.

Meneveau, C., T. Lund, and W. Cabot, "A Lagrangian Dynamic Sub-grid scale Model of Turbulence," J. Fluid Mechanics., **315** , 353 1996.

Murakami, S., A. Mochida, and K. Matsui " Large Eddy Simulation of non-isothermal room airflow, -comparison between standard and dynamic type of Smagorinsky model-" SEISAN-KENKYU, Journal of Institute of Industrial science, University of Tokyo, **47**(2); 7-12, 1995.

Piomelli, U., W. H. Cabot, P. Moin, and S. Lee, "Subgrid-scale backscatter in turbulent & transitional flows, " J. Physics Fluids A, **3**, 1766 1991.

Zang, Y., R. L. Street, and J. R. Koseff, "A dynamic mixed subgrid-scale model and its application to recalculating flow, " J. Physics Fluids A, **5**, 3186, 1993.